Utah State University
DigitalCommons@USU

CEE Faculty Publications | Civil and Environmental Engineering

2002

# A Probabilistic Approach for Channel Initiation

E. Istanbulluoglu

D. G. Tarboton

Robert T. Pack
*Utah State University*

C. Luce

Follow this and additional works at: http://digitalcommons.usu.edu/cee_facpub

Part of the Civil and Environmental Engineering Commons

Recommended Citation
Istanbulluoglu, E., Tarboton, D.G., Pack, R.T., Luce, C. 2002. A probabilistic approach for channel initiation. Water Resources Research, v.38, n.12, p.1325.

This Article is brought to you for free and open access by the Civil and Environmental Engineering at DigitalCommons@USU. It has been accepted for inclusion in CEE Faculty Publications by an authorized administrator of DigitalCommons@USU. For more information, please contact dylan.burns@usu.edu.

UtahStateUniversity
MERRILL-CAZIER LIBRARY

# A probabilistic approach for channel initiation

Erkan Istanbulluoglu,[1] David G. Tarboton, and Robert T. Pack
Civil and Environmental Engineering Department, Utah State University, Logan, Utah, USA

Charles Luce
Rocky Mountain Research Station, U.S. Forest Service, Boise, Idaho, USA

Received 19 July 2001; revised 13 March 2002; accepted 28 March 2002; published 31 December 2002.

[1] The channel head represents an important transition point from hillslope to fluvial processes. There is a nonlinear threshold transition across the channel head with sediment transport much larger in channels than on hillslopes. Deterministic specific catchment area, $a$, thresholds for channel initiation, sometimes dependent on slope, $S$, in the form of $aS^{\alpha} \geq C$, have been suggested. In this paper the channel initiation problem is viewed probabilistically with a spatially variable probability of channel initiation that depends on slope, specific catchment area, and the probability distributions of median grain size, surface roughness, and excess rainfall rate. The channel initiation threshold $C$ is cast as a random variable to characterize the variability of $aS^{\alpha}$ at channel heads. Using field measurements from the Idaho Batholith, we show that median grain size measurements at each channel head explain a significant part of the observed variability of $aS^{\alpha}$. We then characterize the variability of model inputs (median grain size, roughness, and excess rainfall) using probability distributions and show that the probability distribution of area-slope threshold derived from these inputs matches the probability distribution of area-slope thresholds measured at field channel head locations. A gamma probability distribution provides a reasonable match to the distributions of area-slope threshold measured and modeled at channel heads in our study area and in other published channel head data. *INDEX TERMS:* 1815 Hydrology: Erosion and sedimentation; 1824 Hydrology: Geomorphology (1625); 1886 Hydrology: Weathering (1625); *KEYWORDS:* channel initiation, erosion, sediment transport, probability

**Citation:** Istanbulluoglu, E., D. G. Tarboton, R. T. Pack, and C. Luce, A probabilistic approach for channel initiation, *Water Resour. Res.*, *38*(12), 1325, doi:10.1029/2001WR000782, 2002.

## 1. Introduction

[2] Substantial amounts of sediment are transported from hillslopes to streams due to flow concentration and the incision of channels. The upslope boundary of concentrated water flow and sediment transport between definable banks is called a stream channel head [*Dietrich and Dunne*, 1993]. The channel head has been either regarded as a point of transition in the sediment transport process where incisive wash processes begin to dominate over diffusive processes [*Smith and Bretherton*, 1972] or as a point where incision starts with the exceedance of an erosional threshold [e.g., *Horton*, 1945; *Montgomery and Dietrich*, 1988; *Willgoose et al.*, 1991a, 1991b; *Dietrich et al.*, 1993].

[3] Laboratory, field, and theoretical studies of sediment transport mechanics have concluded that fluvial transport of sediment grains does not occur until a critical shear stress is exceeded [*Shields*, 1936; *Yalin and Karahan*, 1979]. *Horton* [1945] proposed that an erosion threshold controls the location of channel heads. He suggested that the critical distance below the topographic divide required for sheet flow erosion is the same as that required for channel incision. According to Horton's theory, channels as erosion features may expand rapidly upslope in response to changed climate and land use conditions and can even form during individual storm events. Field experiments under rainfall simulation demonstrated that sheet flow is inherently unstable and can easily separate into streams, incise channels, and integrate into a network [*Dunne and Aubry*, 1986]. However, such a tendency can be reversed by raindrop impact, soil creep and other diffusive processes [*Dunne and Aubry*, 1986]. This has also been shown theoretically by *Smith and Bretherton* [1972].

[4] On the basis of field evidence and theory, *Montgomery and Dietrich* [1988, 1989, 1994], *Dietrich et al.* [1993], and *Montgomery* [1994, 1999] discussed the existence of a slope dependent contributing area threshold required to support a channel head. This threshold is similar to Horton's critical distance description for channelization but accounts for channel initiation by saturation overland flow and pore-pressure induced landsliding. *Montgomery and Dietrich* [1992] and *Dietrich et al.* [1993] showed that data from channel heads observed in their Tennessee valley field site fit an inverse relationship between the specific catchment

[1]Now at Department of Civil and Environmental Engineering, Massachusetts Institute of Technology, Cambridge, Massachusetts, USA.

Copyright 2002 by the American Geophysical Union.
0043-1397/02/2001WR000782$09.00

area (upslope contributing area per unit contour width) "$a$" and local slope "$S$" of the form,

$$aS^{\alpha} = C \tag{1}$$

where $\alpha$ is an exponent that varies between 1 and 2 and $C$ is a constant. They found that with $\alpha = 2$, all the channel heads observed are captured between two topographic threshold lines with $C$ values of 25 m and 200 m. This reveals a factor of eight variation in the contributing area sizes required for channel initiation for a given slope in the field. *Montgomery and Dietrich* [1992, p. 828] explained this observation as follows: "This scatter probably arises from both spatial and temporal variation in the hydrologic and erosional processes governing channel initiation and should introduce considerable variation into channel and valley development, thus contributing a random aspect to the appearance of many landscapes." The model was thus generally successful at delineating slope-area bounds for channel head locations but acknowledged scatter due to spatial variations in hydrologic and erosional processes [*Dietrich et al.*, 1993; *Prosser and Dietrich*, 1995; *Prosser and Abernethy*, 1996].

[5] The lack of a distinct topographic threshold at channel heads in the form suggested in the literature was also reported in case of intense gullying due to land use pattern changes [*Prosser and Soufi*, 1998; *Desmet and Govers*, 1997]. *Desmet et al.* [1999] experimented with different area exponents in equation (1) to see how they could best match grid cells observed to be gullied in the field to grid cells predicted to be gullied, while setting the threshold $C$ to keep the fraction of area mapped as gullies roughly constant. Their best results classified 70 to 80% of grid cells correctly, although this success does depend on their threshold $C$ and does not consider the number of grid cells in excess of the threshold not considered to be gullied.

[6] Erosion is highly nonlinear with threshold functionality or dependence upon the occurrence of channelization. A model that uses a single channel initiation threshold based on average or central tendency parameters will predict significant erosion only in locations where channelization is predicted on a long-term basis. The work cited above has indicated the presence of variability in the channel initiation threshold and the need for a model that explicitly recognizes this variability. Here we take the logical next step of formalizing the description of this variability by interpreting the threshold $C$ as a random variable, with probability distribution derived physically from the random variability of quantities involved in the erosion process. This description of channel initiation incorporates higher frequency temporary excursions of channelization into terrain that is on the average not channeled over longer timescales. Estimating sediment transport rates from hillslopes is important during extreme rainfall events, when ephemeral rills and gullies are formed. In this study the question of how to parameterize the variability of relevant hydraulic and hydrologic hillslope properties used deterministically in the previous models has been studied and a probabilistic approach to channel initiation has been developed. Our probabilistic model, recognizing the uncertainty and spatial as well as temporal variability in its parameters, predicts a contribution to erosion (represented probabilistically) due to channelization even at locations that do not meet the central tendency channelization threshold. It is our premise in this paper that this new approach provides further insights into the role of uncertainty in the prediction of erosion for soil management purposes.

[7] In what follows we first develop a theory of channel initiation that expresses the probability of channel initiation in terms of the randomness of channel initiation threshold $C$ derived from primary random inputs of sediment size, additional roughness (roughness due to vegetation and obstructions) and excess precipitation rate and show its contribution to probabilistic representation of erosion and sediment transport. This theory assumes the initiation of channels where shear stress exceeds a critical value [*Dietrich and Dunne*, 1993] and develops the probability distribution for this occurrence. The theory can be used to map the probability of channel initiation both for a single channel forming runoff event and integrating over a range of events in time as long as appropriate probability distributions are used to characterize the model inputs. The single event approach, which emphasizes spatial variability, is used in this paper to test the concept through comparison to observed gully initiation from a single storm. The integrated approach that incorporates both spatial and temporal variability is most appropriate for practical management applications, but is less easily tested directly, so we suggest justification of the integrated approach based upon the results from single event tests.

[8] We then describe our field area where the channel heads were mapped and median sediment size, $d_{50}$, was measured at each channel head. We test the theoretical relationship between $d_{50}$ and channel initiation threshold. Finally we select reasonable probability distributions for the other random inputs to $C$ and compare the probability distributions of derived $C$ to the probability distributions of observed $aS^{\alpha}$ at channel heads. We show that the distribution of derived $C$ is well approximated by a gamma distribution, and that a similar gamma distribution matches the distribution of area slope observations in other published channel head data.

## 2. Probabilistic Approach for Channel Initiation

[9] The total shear stress associated with overland flow is

$$\tau_t = \rho_w g y S \tag{2}$$

where, $\rho_w$ is the density of water, $g$ gravitational acceleration, $y$ is the flow depth, and $S$ is the sine of the slope angle. Effective shear stress acting on the bare soil surface is a portion of $\tau_t$ due to shear stress partitioning between vegetation, soil and other roughness elements such as obstructions and surface irregularities [*Foster et al.*, 1989]. The effective shear stress, $\tau_f$ acting on the bare soil surface can be approximated by [*Tiscareno-Lopez et al.*, 1994]

$$\tau_f = \tau_t \left( \frac{n_b}{n_a + n_b} \right)^{1.5} \tag{3}$$

where, $n_b$ is Manning's roughness coefficient for bare soil and $n_a$ is additional roughness due to vegetation, obstructions and surface irregularities [*Arcement and Schneider*, 1984]. Bare soil roughness can be explicitly related to median sediment diameter, $d_{50}$. Many empirical relationships presented for $n_b$ have a general form [*Yen*, 1992]

$$n_b = k d_{50}^{p} \tag{4}$$

where $k$ is a constant and $p = 1/6$. We used $k = 0.0474$, the value proposed by Strickler for sand [see *Yen*, 1992]. In this relationship $d_{50}$ is expressed in m. This equation has been used for overland flow [*Julien and Simons*, 1985]. With the $d_{50}$ values we observed in the field this relationship gives values for $n_b$ in the range 0.01 to 0.03 consistent with the range of $n_b$ values for sand and gravel suggested for overland flow routing by *Woolhiser et al.* [1990] and *Engman et al.* [1986].

[10] Using laboratory and field data and some data from the literature *Rouhipour et al.* [1999] showed that Manning's equation gives more accurate estimates of overland flow velocity than the Darcy-Weisbach and Chezy equations. Assuming uniform overland flow, the depth $y$ in equations (2) from Manning's equation is

$$y = \left[(n_b + n_a)q_o/S^{1/2}\right]^{3/5} \tag{5}$$

where, $q_o$ is the overland flow per unit contour width. Substituting equation (5) into equations (2) and (3), the effective shear stress can be written as

$$\tau_f = \beta_1 q_o^{m_1} S^{n_1} \tag{6}$$

where, $m_1 = 0.6$, $n_1 = 0.7$ and $\beta_1 = \rho_w g n_b^{1.5}(n_b + n_a)^{-0.9}$. If we assume that overland flow incises a channel when $\tau_f$ exceeds a critical channel initiation shear stress threshold, $\tau_c$, then a channelization threshold would be

$$\beta_1 q_o^{m_1} S^{n_1} \geq \tau_c \tag{7}$$

[11] We consider two models for runoff generation to estimate $q_o$ in equations (6) and (7). The first model assumes that $q_o$ is proportional to the specific catchment area, $a$, as

$$q_o = ra \tag{8}$$

where $r$ is the net water input rate (rainfall or snowmelt minus evaporation and infiltration). This we term "infiltration excess" because $r$ is the precipitation in excess of infiltration independent of topography. Substituting equation (8) into equation (7) and rearranging gives

$$aS^{\alpha} \geq C \tag{9}$$

where $\alpha = n_1/m_1 = 1.167$ and $C$ is an area-slope threshold for channel initiation similar to the form suggested previously [*Willgoose*, 1989; *Dietrich et al.*, 1993] given by

$$C = \left(\frac{\tau_c}{\rho_w g n_b^{1.5}(n_b + n_a)^{-0.9} r^{m_1}}\right)^{1/m_1} \tag{10}$$

With the positive value for $\alpha$, equation (9) predicts a negative relationship between slope and drainage area for constant $C$ at channel heads.

[12] The second model for runoff generation assumes a limited lateral transport capacity in the soil profile equal to slope times transmissivity, $TS$. Overland flow is assumed to occur when this capacity is exceeded and is equal to the surface water input in excess of the lateral transport capacity;

$$q_o = ra - TS = r(a - a_s), a > a_s \tag{11a}$$

where,

$$a_s = ST/r \tag{11b}$$

is the specific catchment area required for saturation under steady state conditions and $T$ is the transmissivity of soil profile. This is a saturation excess model for runoff generation similar to the topography-based model of catchment hydrology, TOPMODEL [*Beven and Kirkby*, 1979]. Runoff occurs only for locations where the wetness index $a/S$ exceeds a threshold, here equal to $T/r$.

[13] Using the relationships in equations (7) and (11), the threshold for channel initiation for saturation excess overland flow can be written as

$$(a - a_s)S^{\alpha} \geq C \tag{12}$$

With this model the drainage area required to support runoff increases with slope. This can lead to a positive area-slope relationship for constant $C$ at channel heads [*Montgomery and Dietrich*, 1994; *Montgomery*, 1999].

[14] Our model assumes channel initiation when the shear stress required to initiate sediment transport (incipient motion or detachment) from the bare soil surface is exceeded. This, through equation (10) gives the channelization threshold, $C$. The critical shear stress, $\tau_c$, that goes into equation (10) is estimated from *Shields'* [1936] equation as

$$\tau_c = \tau^* g(\rho_s - \rho_w)d_{50} \tag{13}$$

where, $\tau^*$ is the dimensionless critical shear stress for incipient motion or detachment of particles with the median grain size, $d_{50}$, and $\rho_s$ is the sediment density. For rough turbulent flows an average value of $\tau^* \cong 0.045-0.046$ [*Gessler*, 1971; *Miller et al.*, 1977; *Yalin and Karahan*, 1979]; $\tau^*$ may also be obtained from the Shields diagram using the shear Reynolds number,

$$R^* = u^* \frac{d_{50}}{\nu} = \sqrt{\tau_t/\rho_w}\frac{d_{50}}{\nu} = \sqrt{gyS}\frac{d_{50}}{\nu} \tag{14}$$

where $\nu$ is the kinematic viscosity and equation (2) has been used to obtain the right-hand expression. When $\tau^*$ is evaluated using this approach it depends on $r$ and topographic variables $a$ and $S$. However, this dependence is weak. We simulated a range of $a$, $S$, and $r$ values representative of the terrain and effective rainfall in our field site and found that $\tau^*$ ranged narrowly between 0.04 and 0.046, so selected $\tau^* = 0.043$ for the remainder of this work. This has the advantage of keeping the channel initiation threshold $C$ independent of topographic variables making for more meaningful comparisons with $aS^{\alpha}$ at channel heads. There may in fact be a wider range in $\tau^*$ values for rough turbulent flows [*Buffington and Montgomery*, 1997] that will likely contribute to the variability of channel heads observed in the field. However, $\tau^* = 0.043$ is consistent with the $\tau^*$ values reported by [*Buffington and Montgomery*, 1997] for coarse sand and fine gravel observed in our field areas.

[15] The left-hand sides of equations (9) and (12) include topographic variables which can be derived from digital elevation models (DEMs) using algorithms to evaluate local slopes and specific catchment areas such as from *Tarboton* [1997]. The $C$ parameter on the right hand side of (9) and (12) absorbs all the other hydrologic and geomorphic parameters. Obtaining proper values for $C$ may require field studies and experiments as well as remote sensing analysis. However, even under a fixed land use condition or geological setting the parameters absorbed by $C$ may show

significant variability in space and time, particularly in the case of $r$. To account for this we assume spatially homogenous probability distributions for $d_{50}$, $n_a$, and $r$, which are used to calculate $C$ in equation (10). To simplify matters we ignore variability of r within the area contributing to each point and thus assume that equations (8) and (11) hold for each specific realization of random $r$. This assumption lets us characterize both spatial and temporal variations of the area-slope threshold $C$. The scheme to derive a probability distribution for $C$ and to calculate probability of channel initiation over the terrain is shown in Figure 1. Figure 1 depicts the terrain inputs $S$ and $a$, which are combined to $aS^{\alpha}$ and random inputs $d_{50}$, $r$, and $n_a$. We selected $d_{50}$ as a random variable, because it can be used to estimate both $n_b$ and $\tau_c$ from equations (4) and (13), respectively, and it can be measured in the field. Once $n_b$ is estimated from $d_{50}$, then possible ranges of additional Manning's roughness, $n_a$ can be obtained from tables of total Manning's roughness ($n_b$ + $n_a$) coefficients for overland flow based on land use conditions [e.g., *Engman*, 1986; *Woolhiser et al.*, 1990]. The quantities $\tau_c$, $n_b$, $n_a$, and $r$ are combined through equation (10) to obtain $C$. This figure amounts to a Bayes net for estimating the probability distribution of $C$ given uncertainty in the inputs $d_{50}$, $r$, and $n_a$, characterized by probability distributions. For the infiltration excess overland flow model, the spatial probability of channel initiation (PCI) of a given location can be described by the probability of channel initiation threshold $C$ being less than or equal to $aS^{\alpha}$ calculated from the terrain, formalized as

$$PCI^{ie} = P(C \le aS^{\alpha}) = \int_0^{aS^{\alpha}} f_C(C)dC \qquad (15)$$

where $f_C(C)$ is the probability density function of $C$. Evaluating the probability of channel initiation for saturation overland flow is more complex than that of infiltration excess because it involves the parameter as $T/r$, which should also vary randomly because of the randomness in $r$, and perhaps also $T$. First, we write equation (12) in the form of equation (9) as

$$aS^{\alpha} \ge B + C \qquad (16)$$

where $B = S^{\alpha+1}T/r$. Here we have the addition of two related random numbers. Let $C' = B + C$, then the probability density function for $C'$, $f_{C'}(C')$, can be evaluated at each location and integrated to give the probability of channel initiation due to saturation excess overland flow

$$PCI^{se} = P(C' \le aS^{\alpha}) = \int_0^{aS^{\alpha}} f_{C'}(C')dC' \qquad (17)$$

[16] *Barling et al.* [1994] indicated that the steady state assumption originating in TOPMODEL and expressed here in equations (8) and (11) has some limitations. They calculated specific catchment area as a function of rainfall duration (partial contributing area). This idea may be implemented by using a partial contributing area in equations (15) and (17). In general we expect that the partial contributing area should be a function of water input duration, $D$, and so would use $a(D)S^{\alpha}$ as the upper limit in the integral of equations (15) and (17).

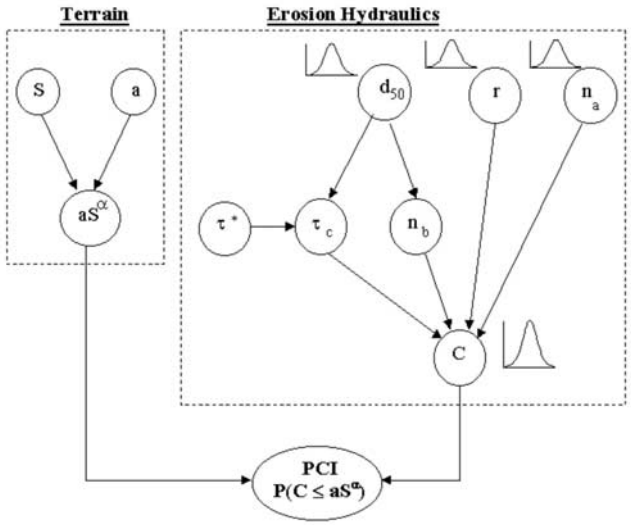


**Figure 1.** Information flow network used to derive a probability distribution for channel initiation threshold $C$ and to calculate the probability of channel initiation (PCI) over the terrain.

[17] We have not derived functional forms for the probability distributions of PCI given by equations (15) and (17). Instead, we use Monte Carlo simulation to generate samples of $C$ for the numerical evaluation of PCI. We show numerically that the results from this Monte Carlo simulation can be approximated using a gamma distribution.

[18] Equations (15) and (17) express the probability of channel initiation at each point conditional on probability distributions of the inputs, namely, sediment size, additional roughness, and runoff rate. The sediment size and additional roughness are spatial probability distributions. Only one realization of these will actually exist in any given landscape. However, the specific spatial pattern of sediment size and additional roughness is practically unobservable so the probability distributions quantify the uncertainty in knowing this information. Additional roughness, in part due to vegetation may also be affected by land management activities. Effective runoff on the other hand is both spatially and temporally variable and for practical applications should be quantified using a probability distribution for representative extreme events over a design period. The PCI concept can then, when coupled with local detachment (erosion) and the sediment transport models, and integrated spatially express the aggregate expected value of erosion. This integrated estimate may be non zero as long as the PCI is greater than zero somewhere in the area, even though a threshold erosion model may have predicted no erosion due to channel incision because the single average or central tendency erosion threshold was not exceeded.

## 3. Field Study

### 3.1. Setting

[19] The above-described methodology has been applied in the Idaho Batholith and its ability to characterize the probability distributions of observed $C$ at channel head locations has been tested. This area consists of an extensive

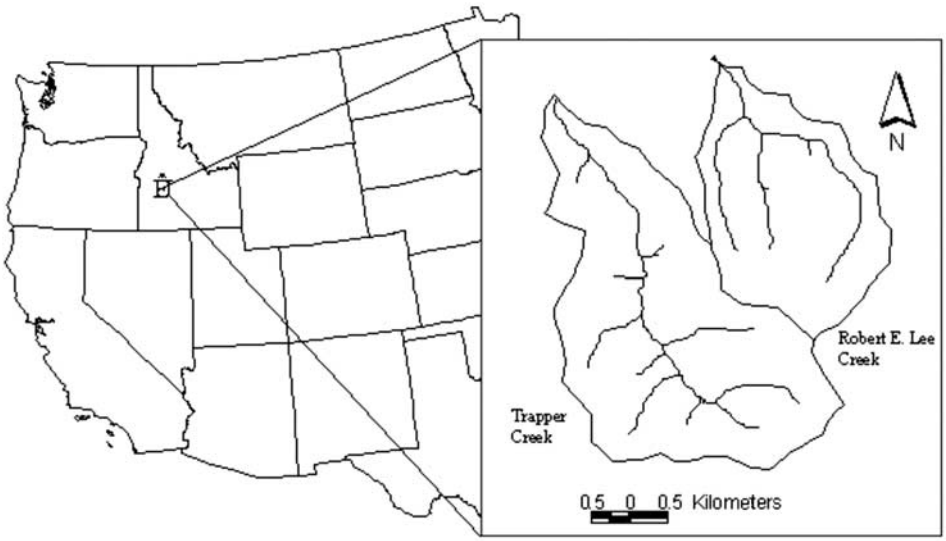


**Figure 2.** Location map of the field sites.

mass of granitic rock (16,000 miles$^2$) that covers a large portion of Idaho and some parts of Montana. It is almost entirely mountainous and forested. Extremely erodible coarse textured soils are found on steep gradients that often exceed 70% [*Megahan*, 1974]. Average annual precipitation is approximately 1000 mm. Localized high-intensity rainstorms of short duration are common during summer. At other times of the year low-intensity storms with longer durations occur, often in conjunction with snowmelt. Following soil disturbance, the combination of steep topography, high soil erodibility, and high climate stress often results in accelerated surface erosion [*Megahan and Kidd*, 1972]. The specific study areas selected are Trapper and Robert E. Lee Creeks within the North Fork of the Boise River in southwestern Idaho (see Figure 2). Trapper Creek was intensely burned by a wildfire in 1994, and extreme gullying was initiated by a convective summer storm in 1995, possibly due to water repellent conditions of the surface soil. The gullies generated by this storm are probably ephemeral channels but, nevertheless, resulted in considerable erosion. Robert E. Lee (REL) Creek was partially burned to a light to moderate degree. Although REL Creek is adjacent to Trapper Creek, intense gullying did not occur in REL Creek, presumably because of either higher infiltration capacity from less water repellency or lower localized rainfall intensities or a combination of both these effects.

### 3.2. Field Observations

[20] A limited data set of channel head locations was collected using the definition of the channel head as the upstream limit of observable erosion and concentration of flow within definable banks [*Montgomery and Dietrich*, 1989]. Channel heads in Trapper Creek have head cuts of 0.3 m to 1m in width and an average of 0.5 m depth. Some head cuts were even observed at the ridge crest. Local slopes (over a length of 10 to 20 m) at the channel heads were measured in the field using a Suunto inclinometer and a GPS was used to record locations. Sediment size samples were collected just above the head cuts to approximate the sediment size in transport when the incisions occurred. These samples were sieved and the median size of each sample was determined. Contributing areas were derived from the 30 m DEM of the study site using the D$\infty$ algorithm [*Tarboton*, 1997]. Contributing area was also checked in a few channel head locations by hiking perpendicular to what was judged to be the elevation contours, from both sides of the channel heads. This data for Trapper Creek is presented in Table 1.

[21] Channels in Trapper Creek were usually discontinuous and faded out downstream from the most upstream limit of erosion within definable banks, with sequential head cuts occurring downslope. In these cases we also recorded the locations of the most downslope head cut, which we term the head of the continuous channel. Starting from the heads of the continuous channels, slopes were measured in the field at intervals from 20 to 40 m for distances ranging between 150 m and 500 m downslope. GPS was used to record the slope measurement locations and contributing areas were again derived from the 30 m DEM of the study site using the $D\infty$ algorithm [*Tarboton*, 1997].

[22] We do not know the rainfall rate of the storm that incised the channels in Trapper Creek. However, some forest service personnel were exposed to that storm and they estimated that more than 2.54 cm (1 inch) of rain fell in less than half an hour. It is conceivable that this kind of a convective storm event could result in local intensities of between 50 mm/h and 100 mm/h.

[23] Two distinct types of channel heads were observed in REL Creek. We observed channel incisions because of saturation excess overland flow (SEOF) where fire effects were insignificant. The vegetation mat was broken mostly by seepage forces and sediment entrained by saturation overland flow. These channel heads support gravel bed streams with definable banks stabilized by vegetation. Infiltration excess overland flow (IEOF) channel incisions were observed where there is disturbance by light to moderate fire or forest harvest or there is bedrock exposure and coarse materials such as cobbles and rock fragments

**Table 1.** Observed Specific Catchment Area, Slope, and Median Grain Size at Channel Head Locations in Trapper Creek and Calculated Parameters Required to Estimate Channel Initiation Threshold, *C*, and Calculated *C* Values at Each Location

| Observed | | | Calculated | | | | |
|---|---|---|---|---|---|---|---|
| Specific Catchment area, m | Slope, m/m | $d_{50}$, [a] mm | $aS^{\alpha}$, m | $n_b$ | $n_t$ | $\tau_c$, Pa | |
| 100 | 0.42 | 1.700 | 33.1 | 0.0164 | 0.0684 | 1.17 | 15.48 |
| 30 | 0.32 | 1.700 | 7.5 | 0.0164 | 0.0684 | 1.17 | 15.48 |
| 30 | 0.23 | NA | 5.2 | | | | |
| 46 | 0.40 | 2.000 | 14.5 | 0.0168 | 0.0688 | 1.38 | 19.15 |
| 125 | 0.72 | NA | 66.8 | | | | |
| 30 | 0.31 | 1.300 | 7.3 | 0.0157 | 0.0677 | 0.89 | 10.90 |
| 40 | 0.25 | 1.330 | 7.7 | 0.0157 | 0.0677 | 0.91 | 11.23 |
| 61 | 0.45 | NA | 21.6 | | | | |
| 67 | 0.45 | NA | 23.7 | | | | |
| 123 | 0.45 | 2.200 | 43.5 | 0.0171 | 0.0691 | 1.51 | 21.71 |
| 56 | 0.30 | 1.630 | 13.1 | 0.0163 | 0.0683 | 1.12 | 14.65 |
| 53 | 0.39 | 2.000 | 16.3 | 0.0168 | 0.0688 | 1.38 | 19.15 |
| 72.7 | 0.42 | NA | 24.0 | | | | |
| 30 | 0.23 | 1.600 | 5.2 | 0.0162 | 0.0682 | 1.10 | 14.30 |
| 68 | 0.41 | 2.380 | 21.9 | 0.0173 | 0.0693 | 1.64 | 24.06 |
| 45 | 0.32 | 2.250 | 11.3 | 0.0172 | 0.0692 | 1.55 | 22.35 |
| 30 | 0.31 | NA | 7.3 | | | | |
| 68 | 0.60 | 2.200 | 31.3 | 0.0171 | 0.0691 | 1.51 | 21.71 |
| 57 | 0.46 | 1.750 | 20.6 | 0.0165 | 0.0685 | 1.20 | 16.08 |
| 59 | 0.53 | 2.730 | 24.3 | 0.0177 | 0.0697 | 1.88 | 28.81 |
| 40 | 0.30 | 1.700 | 9.3 | 0.0164 | 0.0684 | 1.17 | 15.48 |
| 32 | 0.40 | 2.100 | 10.1 | 0.0170 | 0.0690 | 1.44 | 20.42 |
| 60 | 0.49 | NA | 23.0 | | | | |
| 139 | 0.67 | NA | 70.2 | | | | |
| 103 | 0.53 | 2.900 | 42.5 | 0.0179 | 0.0699 | 1.99 | 31.19 |
| 70 | 0.35 | 1.600 | 19.2 | 0.0162 | 0.0682 | 1.10 | 14.30 |
| 88 | 0.40 | 2.900 | 27.7 | 0.0179 | 0.0699 | 1.99 | 31.19 |

[a]NA indicates sediment size distribution data are not available.

on the surface. There was not significant vegetation cover around IEOF channel heads in REL Creek and channels were ephemeral discontinuous small gullies. The channel heads located on hillslopes where there is coarse surface material, rock fragments or exposed bedrock were separated in the model analysis because the percentage of rock was not quantified in our field measurements limiting our ability to use methods that account for rock percentage [*Abrahams and Parsons*, 1991; *Nearing et al.*, 1999].

## 4. Pointwise Comparison of the Observed $aS^{\alpha}$ and Calculated C at Channel Heads

[24] The theory developed above suggested that variations in $d_{50}$, $n_a$, and $r$ are responsible for the variation in $aS^{\alpha}$ at channel heads. Here the measured values of $d_{50}$ in Trapper Creek are used to test the contribution of $d_{50}$ to this variability. We set $\alpha = 1.167$ following equation (9). We also set $r = 35$ mm/h in the infiltration excess runoff model assuming about 50% infiltration due to the water repellency remaining a year after the wildfire and rainfall around 70 mm/h in the range 50 to 100 mm/h reported for the channel forming storm. We adjusted $n_a$ to optimize the fit of $C$ values to $aS^{\alpha}$ and obtained $n_a = 0.052$. This is within the range from 0.04 to 0.12 reported by *Woolhiser et al.* [1990] and *American Society of Civil Engineers* [1996] for sparse vegetation and surface litter.

[25] Table 1 includes values of $aS^{\alpha}$ calculated at each observed channel head and $\tau_c$ estimated from $d_{50}$ using equation (13). This $\tau_c$ is used with equation (10) to evaluate $C$. Figure 3 plots $C$ versus observed $aS^{\alpha}$. The regression $R^2$ and Nash-Sutcliff error measure [e.g., *Gupta et al.*, 1998]

$$NS = 1 - \frac{\sum_{i=1}^{n} \left(C_i - aS_i^{\alpha}\right)^2}{\sum_{i=1}^{n} \left(aS_i^{\alpha} - \overline{aS^{\alpha}}\right)^2} \tag{18}$$

indicate that about 40% of the variability in observed $aS^{\alpha}$ may be attributed to $d_{50}$. A similar fit can be obtained for different $r$ values by adjusting $n_a$ with both $r$ and $n_a$ still being within the range of their uncertainty.

## 5. Comparison of Channel Initiation Probability Distributions

[26] The pointwise comparison shown in Figure 3 revealed uncertainties associated not only with $d_{50}$ but also

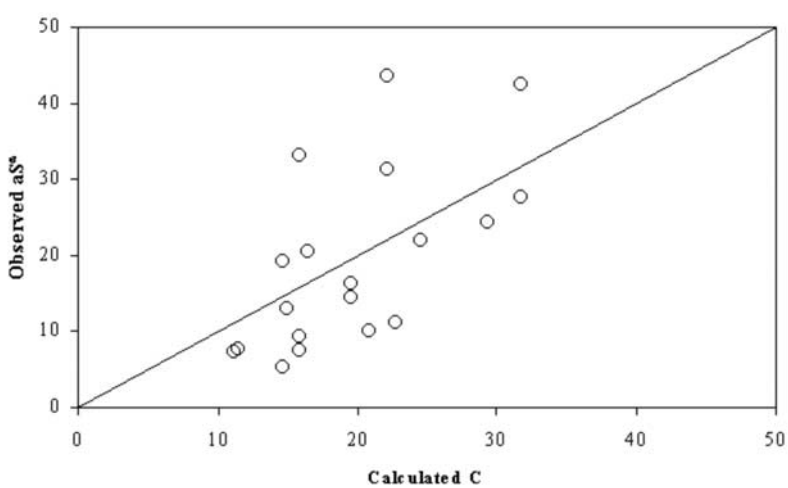


**Figure 3.** Plot of calculated $C$ versus the observed $aS^{\alpha}$ for channel heads in Trapper Creek. Straight line is the 1:1 line. $R^2 = 0.387$ and NS = 0.377.

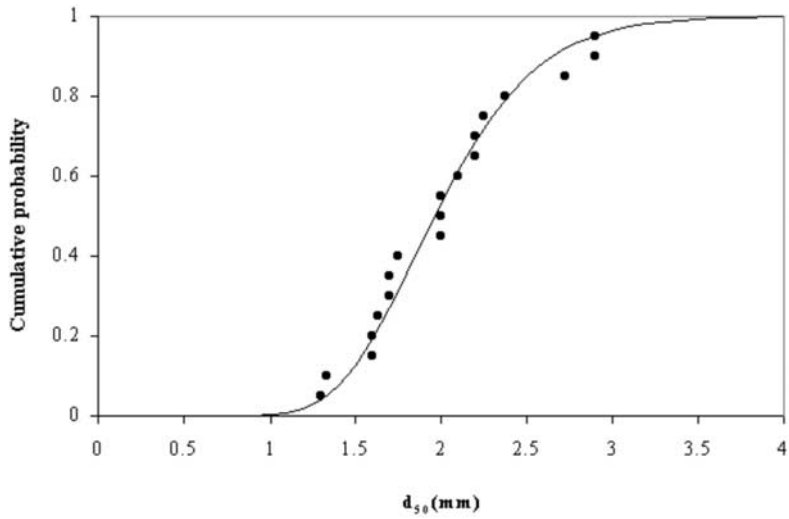


**Figure 4.** Lognormal distribution (solid line) fitted to the cumulative distribution of the median sediment size, $d_{50}$, measurements from Trapper Creek at channel heads estimated by using the Weibull plotting position.

with $r$ and $n_a$. Here we employed the scheme given in Figure 1 to derive a probability distribution for $C$ by Monte Carlo Simulation and compare the derived distribution with the $aS^{\alpha}$ distribution observed at channel heads in the field. This is a single event test of the PCI concept with probability distributions of the inputs chosen as estimates of the single 1995 event responsible for initiation of the channels mapped.

[27] We found that the $d_{50}$ data from Trapper Creek presented in Table 1 was well described by a lognormal distribution with mean $d_{50}$ = 2 mm and standard deviation of 0.48 mm (Figure 4). Uniform distributions were used for the other two input variables, with $r$ between bounds of 15 and 55 mm/h and $n_a$ between bounds of 0.015 and 0.1. These distributions quantify the uncertainty associated with this single event in a simple way. In management applications that integrate over time, other distributions may be more appropriate, specifically for $r$. Fifteen hundred random values for $d_{50}$, $r$, and $n_a$ were generated. Figure 5 compares the cumulative distribution of the simulated $C$ to the cumulative distribution of the observed $aS^{\alpha}$ for channel heads observed in Trapper Creek. The bounds in the probability distributions for $r$ and $n_a$ have been adjusted by trial and error to achieve this fit but are well within the range that is plausible. The field observed channel head $aS^{\alpha}$ have an average, standard deviation and skewness of 26 m 18.4 m and 1.13. The same statistics obtained for $C$ from the Monte Carlo simulation scheme are 26 m, 18.5 m, and 1.56, respectively. Both the simulation statistics and the cumulative distribution of the simulated $C$ show good

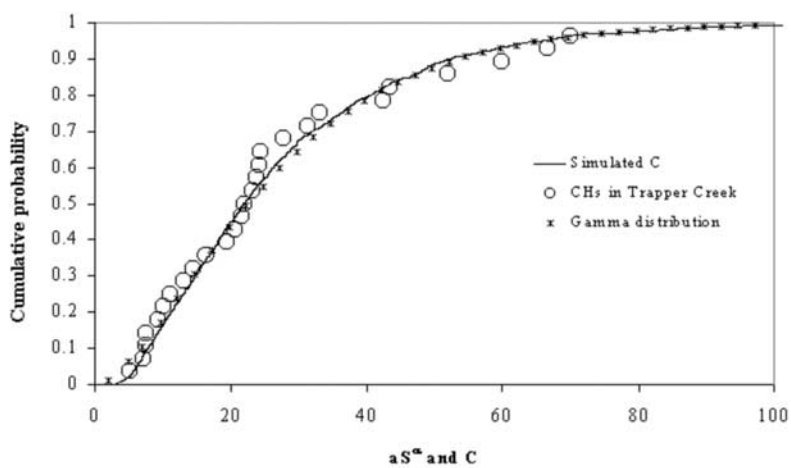


**Figure 5.** Comparison of the cumulative distribution from the simulations of $C$ to the cumulative distribution of observed $aS^{\alpha}$ at channel heads in Trapper Creek and gamma distribution fitted to the observed $aS^{\alpha}$. CDFs are by Weibull plotting position.

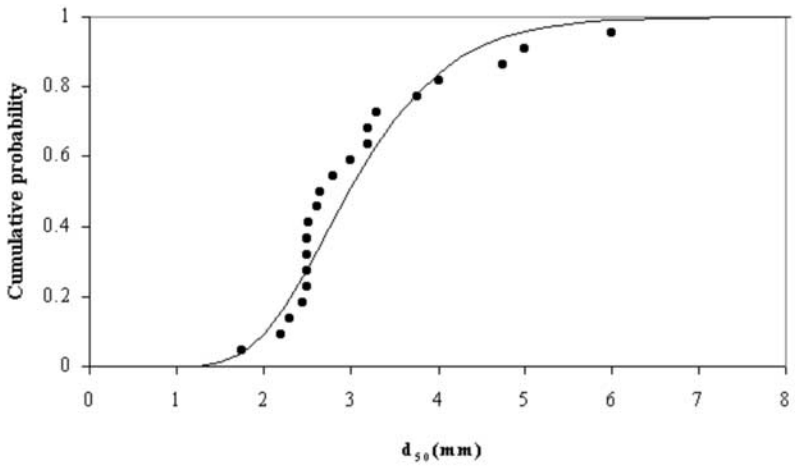


**Figure 6.** Lognormal distribution (solid line) fitted to the cumulative distribution of the median sediment size, $d_{50}$, measurements from REL Creek estimated by using the Weibull plotting position.

correspondence with the observed $aS^{\alpha}$ variability in the field.

[28] Two distinct channel initiation processes, IEOF and SEOF, were observed in REL Creek. We found that the $d_{50}$ data set collected from REL Creek at sites where the channel heads were observed can be fit by a lognormal distribution (Figure 6). The measured $d_{50}$ data have a mean and standard deviation of 3.12 mm and 1.05 mm, respec-

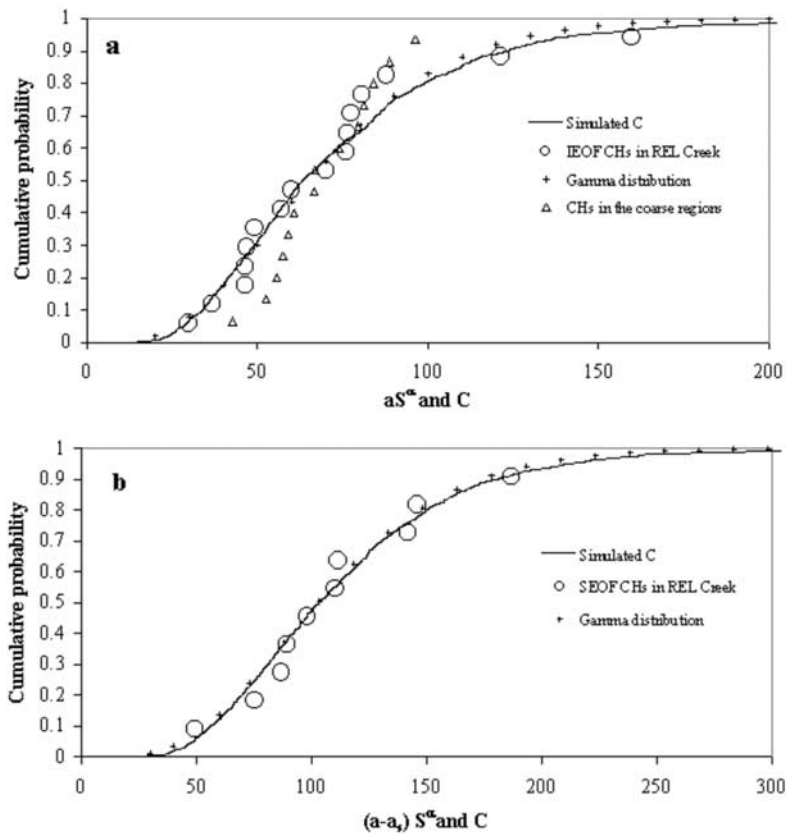


**Figure 7.** Comparison of the cumulative distribution from the simulations of $C$ to the cumulative distribution of observed $aS^{\alpha}$ at channel heads in REL Creek and gamma distribution fitted to the observed $aS^{\alpha}$. (a) Infiltration excess overland flow (IEOF) channel heads (CH). (b) Saturation excess overland flow (SEOF) channel heads. CDFs are by Weibull plotting position.

tively. These numbers are larger than for Trapper Creek. REL Creek soils were generally coarser than Trapper Creek. The lognormal distribution (Figure 6) is used for both IEOF and SEOF channel initiation processes in REL Creek to characterize the $d_{50}$ variability. Uniform distributions were used for the other two inputs $r$ and $n_a$. We used $r$ between bounds of 20 and 30 mm/h and $n_a$ between 0.043 and 0.1 to estimate the PCI for IEOF channel heads. Comparison of the cumulative distributions of the simulated $C$ and the observed $aS^{\alpha}$ for IEOF channel heads in REL Creek is given in Figure 7a. The average, standard deviation, and the skewness of the field observed $aS^{\alpha}$ of the IEOF incisions in REL Creek were 70 m, 33, m and 1.5, respectively. The same statistics obtained from the model are 73 m, 39 m, and 1.7. Since the locations in the REL Creek where IEOF channel heads were observed were lightly burned compared to Trapper Creek, our calibrations of $r$ and $n_a$ are consistent with lower runoff rates (higher infiltration or less intense rainfall) and slightly higher additional roughness values (more vegetation) in those sites.

[29] The IEOF channel heads shown in Figure 7a (as circles) do not include those where coarse surface material, rock fragments and bedrock exposure was observed. Instead, the probability distribution of these is shown separately (as triangles) in Figure 7a. Apart from two points at the high end of the distribution all these channel heads with coarse material, rock fragments, and exposed bedrock lie to the right of the $aS^{\alpha}$ distribution from the other more sandy locations, consistent with the idea that there is a higher critical shear stress threshold at these locations.

[30] At most of the locations of SEOF channel heads saturation and exfiltration was observed in the field without any significant sediment detachment around the channel heads. Equation (11b) gives the specific catchment area required for SEOF. In this equation a value of $T/r$ = 900 m defines a zone of saturation that just includes all the SEOF channel head locations that we mapped. This provides an upper bound on $T/r$ because a finite increment of flow is required to initiate sediment detachment around the channel heads. We modeled the saturation excess channel initiation process assuming a constant $T/r$ of 600 m in equations (11) and (12). From DEM analysis we saw that this value saturates the axis of the major hollows in the watershed and leaves out most of the IEOF channels where no signs of recent sediment transport were observed. Various combinations of $T$ and $r$ can produce a $T/r$ saturation threshold value of 600 m. For example, a $T$ of 40 $m^2$/d requires a steady state precipitation rate of approximately 0.066 m/d. We analyzed 69 years of available precipitation records in the region and found that a daily rainfall of 0.066 m (66 mm) has a return period of about 80 years. The presence of snow can enhance the surface water input due to snowmelt by the rain on snow effect being added to rainfall inputs. However, there is also leakage from the shallow soil into bedrock fractures common in the area. *Megahan and Clayton* [1986] presented 58 bedrock-saturated hydraulic conductivity tests ranging from 0 to 1.7 m/d with a mean and a median value of 0.175 m/d and 0.02 m/d.

[31] We used a constant $r$ of 0.066 m/d (2.75 mm/h) with $T$ = 40 $m^2$/d to characterize the rainfall plus possible snowmelt minus deep percolation losses and evapotranspiration for the SEOF channel initiation analysis. For comparison *Montgomery* [1994] used $T$ = 65 $m^2$/d in the Oregon coast range and *Dietrich et al.* [1992] used $T$ = 17 $m^2$ in their Tennessee Valley California study area. We used the same lognormal probability distribution for $d_{50}$ from field observations in REL Creek (Figure 6) as was used for the IEOF channel initiation analysis. We selected 0.0135 and 0.006 for the lower and upper bound of the uniform distribution for $n_a$ through calibration. Here the effect of additional roughness ($n_a$) is minor because the vegetation mat was broken by seepage forces in most sites. Figure 7b compares the cumulative probability distributions of the observed $(a\text{-}a_s)S^{\alpha}$ and the simulated $C$ at SEOF channel heads. Since the calibrated additional roughness values are very low, and $r$ and $T$ were held constant, Figure 7b shows how the random variation of median sediment sizes can produce significant variation of channel head locations on the terrain.

[32] In the PCI theory, equations (15) and (17) require the probability density function of $C$. Several parametric probability distributions such as exponential, normal, lognormal and gamma were fitted using the mean and variance of the $aS^{\alpha}$ observed. Among those we found that gamma distribution gave the best correspondence with the observed $aS^{\alpha}$ and simulated $C$ distributions (Figures 5 and 7). The gamma probability density function is given by

$$f_C(C) = \frac{\lambda(\lambda C)^{k-1} e^{-\lambda C}}{\Gamma(k)} \tag{19}$$

where $C$ is the threshold for channel initiation and $\lambda$ and $k$ are the distribution parameters which can be estimated from the mean, $\mu_C$, and variance, $\sigma_C^2$, of the observations using $\mu_C = k/\lambda$ and $\sigma_C^2 = k/\lambda^2$. $\Gamma(\ )$ is the gamma function.

## 6. Sensitivity Analysis

[33] Figure 8 shows the sensitivity of the cumulative distribution of $C$ to the distributions used for $d_{50}$, $r$, and $n_a$. In Figure 8a, cumulative distributions for $C$ were generated holding $d_{50}$ at its minimum observed, mean and maximum observed values but generating $n_a$ and $r$ from their random distributions. Figure 8b shows the cumulative distributions obtained holding $r$ fixed at its lower bound, mean and upper bound values while generating $n_a$ and $d_{50}$ from their random distributions. Figure 8c shows the cumulative distributions obtained holding $n_a$ fixed at its lower bound, mean and upper bound values while generating $r$ and $d_{50}$ from their random distributions.

[34] *Montgomery and Dietrich* [1989] tabulated source areas and slopes at 63 channel heads in their Tennessee Valley California study area. Figure 9 plots the cumulative distribution of $AS^{\alpha}$ for these data and shows that it is also well approximated by a gamma distribution. Note that in this comparison contributing area $A$ in $m^2$ is used rather than specific catchment area because the colluvial fill width given in the Montgomery and Dietrich paper is not the same as contour width in the definition of specific catchment area. We have not attempted to fit parameters to the distributions for $r$, $n_a$, and $d_{50}$ for this area because we have insufficient information to do so. Nevertheless, we present these data as third party data illustrative of varia-

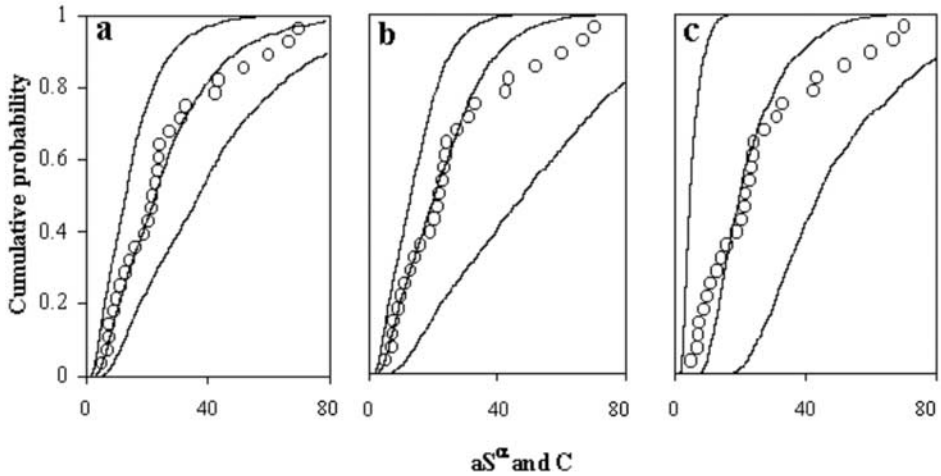


**Figure 8.** Sensitivity of the cumulative distribution of $C$ to the distributions used for $d_{50}$, r, and $n_a$. In Figure 8 curves from left to right are (a) $d_{50}$ = 1.3 mm, $d_{50}$ = 2 mm, and $d_{50}$ = 2.9 mm; (b) r = 55 mm/h, r = 35 mm/h, and r = 15 mm/h; (c) $n_a$ = 0.01, $n_a$ = 0.052, and $n_a$ = 0.1. Circles are the Trapper Creek channel head data.

bility of channel initiation threshold of the same form as predicted by our theory.

[35] Since the gamma distribution fits the data well, we used it in equation (15) to derive a map of PCI over the study watersheds (Figure 10). Here $aS^{\alpha}$ is evaluated at each point from the DEM. PCI is then mapped at each location as the cumulative probability from the incomplete gamma function associated with the $aS^{\alpha}$ value and fitted gamma distribution parameters. The maps show the topographic expression of PCI. Channel head locations towards the upper ends of high PCI zones are consistent with the theory. The PCI values mapped in Trapper Creek correspond to the gamma distribution fitted to observed channel heads (all IEOF) in Figure 5. The PCI values mapped in REL Creek correspond to the gamma distribution fitted to the observed IEOF channel heads in Figure 7a. The different gamma distributions lead to different PCI values for these watersheds, which reflect the effects of the more intense fire in Trapper and increased PCI following the fire.

## 7. Analyzing Hillslope to Channel Transition Using PCI in Slope-Area Diagrams

[36] Slope versus contributing area diagrams are often used to unravel geomorphic processes from DEMs and field observations [*Montgomery and Dietrich*, 1992; *Tarboton et al.*, 1992; *Ijjasz-Vasquez and Bras*, 1995]. In order to show the use of PCI for evaluating the channelization process on slope-area diagrams, Figures 11 and 12 show the slope-area representation of the PCI theory using contours of equal PCI for our study watersheds. The probabilistic approach generates a specific PCI as a function of slope and specific

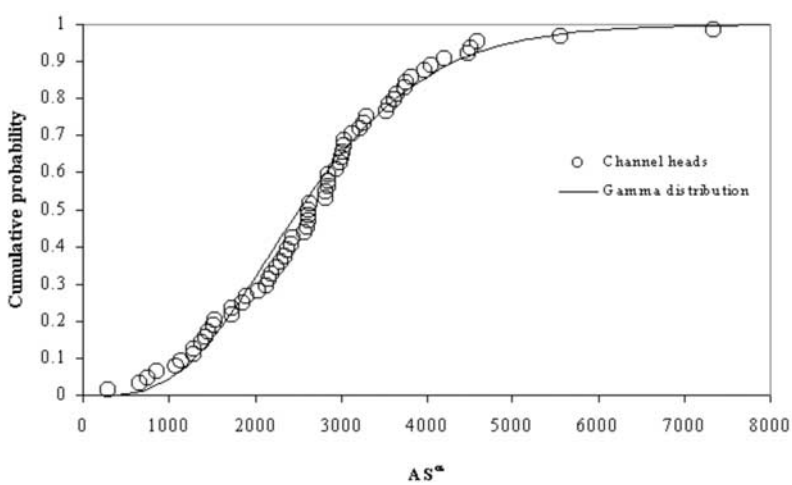


**Figure 9.** Gamma distribution (solid line) fitted to Tennessee Valley channel head data set [*Montgomery and Dietrich*, 1989].

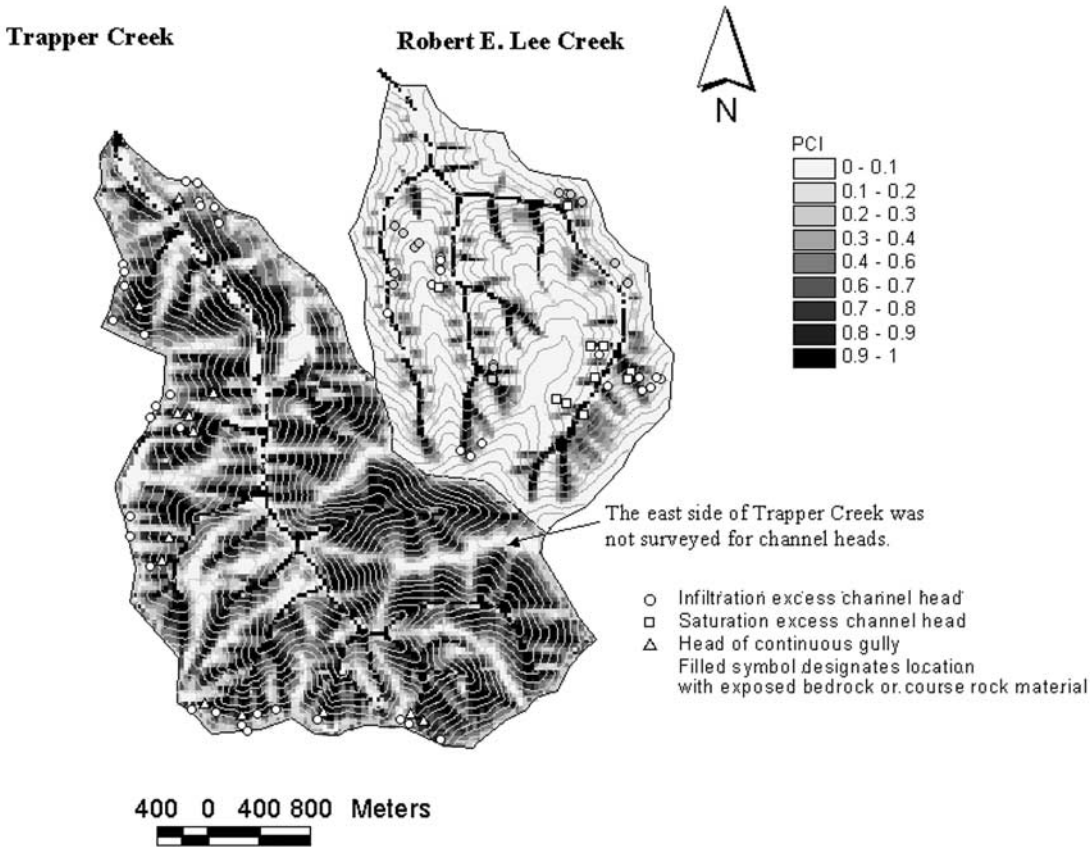


**Figure 10.** Probability of channel initiation (PCI) maps of the study areas derived using the Gamma distribution and mapped channel head locations. Contour interval is 30 m in both watersheds.

catchment area. The probability of channel initiation increases with the increase of either slope or specific catchment area. In Trapper Creek where the heads of continuous channels were mapped separately, we see that heads of observed continuous channels tend to occur in zones with high PCI (the triangles on Figure 11 that occur where PCI > 0.7), while channel heads not associated with continuous channels occur where PCI is lower (circles on Figure 11).

[37] In section 5 we used a T/r = 600 m with equation (11b) to model saturation excess. The line separating saturated from unsaturated areas is shown on Figure 12 (the dashed

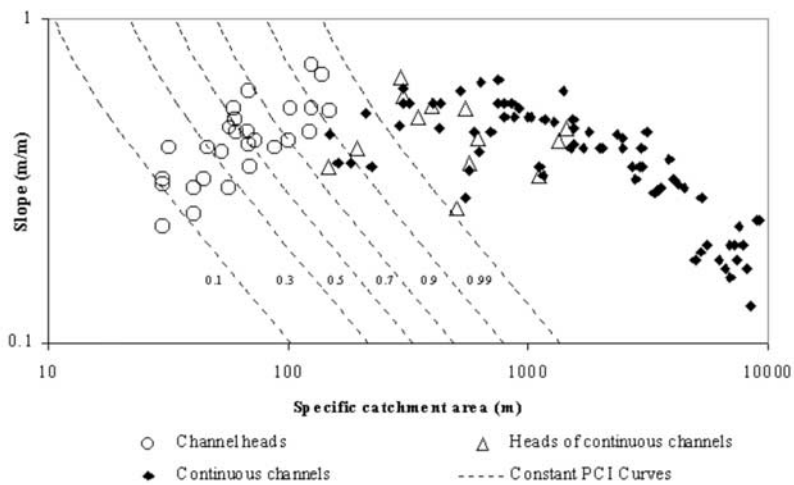


**Figure 11.** Specific catchment area versus local slope plot for channel heads, heads of continuous gullies and gullies observed in Trapper Creek. Dashed lines are the PCI curves from left to right, as labeled.

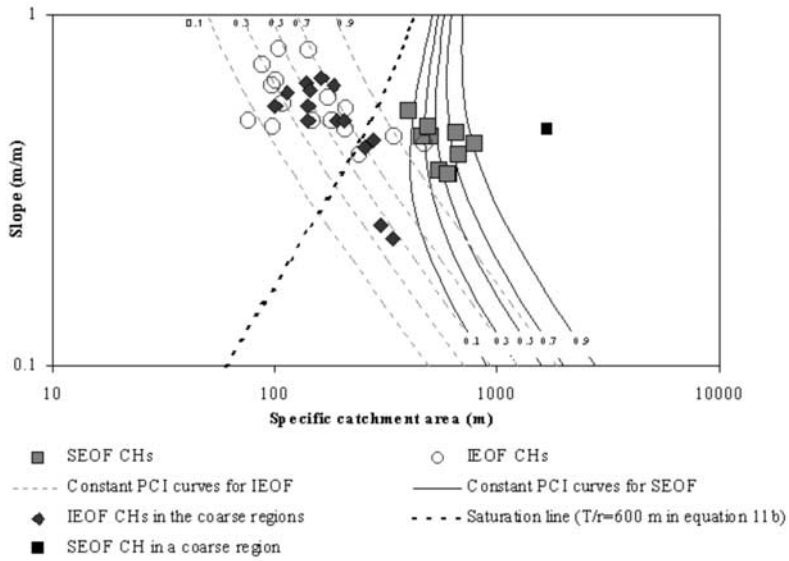


**Figure 12.** Specific catchment area versus local slope plot for channel heads in REL Creek. Lines are the PCI curves from left to right, as labeled.

saturation line) according to this relationship. This separates naturally in slope-area space the channel heads where saturation was observed (SEOF channel heads) from those where saturation was not observed (IEOF channel heads).

## 8. Discussion

[38] Erosion threshold theories for channel initiation [e.g., *Montgomery and Dietrich*, 1988, 1989; *Dietrich et al.*, 1993; *Montgomery and Foufoula-Georgiou*, 1993] have often attributed the observed inverse relationship between the drainage area to support a channel head and the local slope at channel heads to the analytical form of erosion threshold functions such as equation (9). A positive relationship between drainage area and local slope at channel heads can be explained (referring to equations (11) and (12)) in terms of the increase in drainage area required to support runoff with increasing slope in a saturation threshold runoff model [*Montgomery and Dietrich*, 1994]. Both of these effects are seen in Figure 12 where the IEOF constant PCI contours have a negative slope-area relationship and the saturation line and constant PCI contours for SEOF where slope is large have a positive slope-area relationship. We observed (Figure 11) a positive relationship between area and slope at channel head locations in Trapper Creek, but an inverse relationship similar to the previous studies in IEOF channel heads in REL Creek (Figure 12) and a somewhat constant slope with varying specific catchment area in SEOF channel heads in REL Creek. *Prosser and Soufi* [1998] found no clear slope dependency on the drainage area required to support gully heads in intensely gullied hillslopes following land use change.

[39] In interpreting these results we feel that the observed slope-area relationships derived from the topography of landforms and the functional relationship between area and slope derived from the excess-shear stress model with constant threshold are two different concepts. The negative (or positive) slope-area relationships obtained from equality in equations (9) or (12) assume a fixed $C$ at all channel heads, whereas the point of this paper has been to explore spatial and temporal variability in $C$, characterized using probability. Channel formation in equation (9) or (12) requires that at a point, a combination of area and slope should be greater than a certain threshold independent of the morphology of the landscape. Area-slope trends on the topography are established over the long-term evolution of the landscape due to the interactions between diffusive hillslope and fluvial channel processes. Therefore, depending on the $C$ threshold at an instant in time (e.g., a thunderstorm event following a wildfire), channels may erode different hillslope positions where different processes dominate over the long term. If channelization occurs where diffusive processes dominate over the long term (convex hillslopes), then a positive relationship between area and slopes at observed channel heads is expected. The gully heads observed in Trapper Creek after significant disturbance are an example of this effect. Similarly, when channel heads are observed where fluvial sediment transport is dominant (concave valleys), then the area-slope relationship would be negative. One may also observe channel heads in the field where over the long-term diffusive and fluvial processes are in balance. In this case channel head data would reveal no distinct relationship between area and slope. The only case for which channel heads observed in the field may follow the functional form of the relationship between area and slope derived from the shear stress theory is the rather special case where all the model parameters of equation (10) are constant in space and time. In this case an erosional threshold line on area-slope plots would show the transition point between hillslopes and channels [e.g., *Tucker and Bras*, 1998, Figure 11].

## 9. Conclusions

[40] On the basis of the observations presented in this paper, we conclude that channels can incise in different topographic locations depending on the spatial and temporal variability of climate and land cover. The probabilistic

channel initiation zone on the slope-area diagrams shifts back and forth along the specific catchment area axis (compare Figures 11 and 12) depending on the model input values, such as variation of runoff rates and additional roughness due to vegetation cover, that characterize climate and land cover variability.

[41] Flow concentration due to channelization is an important mechanism in erosion and sediment transport. In this paper we have presented a probabilistic theory for modeling channel initiation and tested the theory using field data as an initial step in quantifying this process considering the inherent uncertainties in nature. In this paper we first showed that measured variability of sediment grain size is related to and accounts for a significant portion of the variability in channel initiation threshold observed in the field. We then showed that the probabilistic model developed is capable of producing a probability distribution of channel initiation threshold that matches the observed slope-area dependent channel initiation threshold (Figures 5 and 7). We recognize that probability distributions comparisons are weaker than pointwise comparisons, but have no way to quantify the specific spatial patterns of inputs necessary for more detailed pointwise tests of the model. In the probability distribution comparisons presented, uniform distributions were assumed for some of the inputs. The specific form of these may be questioned. In particular, exponential or gamma distributions are more common distributions used for rainfall. The uniform distribution was used as a convenient noninformative a priori choice. Without specific information it is easy to understand and conceptualize equal likelihood between upper and lower bounds. On the basis of our experimentation, there is sufficient flexibility in the model that it is relatively insensitive to the specific form of the input distribution chosen. It is more important to quantify the variability and uncertainty using some probability distribution rather than worry about the precise form of distribution chosen.

[42] Estimating fluvial sediment transport from hillslopes first requires predicting the channeled portions of the terrain. A model that uses a single channel initiation threshold will predict significant erosion only in locations where channelization is predicted on a long-term basis. Our probabilistic model provides a way to account for the less frequent contribution to erosion due to channelization even at locations that do not meet the single channelization threshold.

[43] The effects of different land management practices on channel initiation and the erosion risk can be visualized by mapping the PCI using DEMs. In forested watersheds, for example, these maps may be useful for spatial planning of forest harvests and developing soil conservation techniques after wildfires. Mapping PCI can also be used in planning land use in agricultural watersheds where the effects of different crop patterns and tillage practices on PCI and the potential for gully erosion is of concern.

[44] The hydrologic response of a basin, such as hydrograph characteristics, is strongly related to geomorphology and climate [*Rodriguez-Iturbe*, 1993]. The closer the channel head is to the watershed divide the longer distance the flow will travel in channels rather than on hillslopes. Expansion of ephemeral gullies to unchanneled hillslopes within a storm event decreases flow travel times within the channel network [*Beven and Wood*, 1993]. Mapping the probability of channel initiation on the terrain (Figure 10) reveals the probabilities of flow transport in both overland and channeled states and contributes to understanding the effects of geomorphologic changes on the hydrologic response of the watersheds.

[45] **Acknowledgments.** We appreciate the thoughtful reviews by David Montgomery and an anonymous WRR reviewer. We are greatly appreciative of financial support from the U.S. Department of Agriculture under contract 9901085 awarded through the Water Resources Assessment Protection Program of the National Research Initiative Competitive Grants Program. We thank field technicians Tom Black and Bernie Riley.

## References

Abrahams, A. D., and A. J. Parsons, Resistance to overland flow on desert pavement and its implications for sediment transport modeling, *Water Resour. Res.*, *27*(8), 1827–1836, 1991.

Arcement, G. J. J., and V. R. Schneider, Guide for selecting Manning's roughness coefficients for natural channels and floodplains, *Rep. RHWA-TS-84-204*, U.S. Geol. Surv., Denver, Colo., 1984.

American Society of Civil Engineers, *Hydrology Handbook*, 2nd ed., *ASCE Manuals Rep. Eng. Pract.*, vol. 28, 784 pp., New York, 1996.

Barling, R. D., I. D. Moore, and R. B. Grayson, A quasi-dynamic wetness index for characterizing the spatial distribution of zones of surface saturation and soil water content, *Water Resour. Res.*, *30*(4), 1029–1044, 1994.

Beven, K. J., and M. J. Kirkby, A physically based variable contributing area model of basin hydrology, *Hydrol. Sci. Bull.*, *24*(1), 43–69, 1979.

Beven, K., and E. F. Wood, Flow routing and the hydrological response of channel networks, in *Channel Network Hydrology*, edited by K. Beven and M. J. Kirkby, pp. 99–128, John Wiley, New York, 1993.

Buffington, J. M., and D. R. Montgomery, A systematic analysis of eight decades of incipient motion studies, with special reference to gravel-bedded rivers, *Water Resour. Res.*, *33*(8), 1993–2029, 1997.

Desmet, P. J. J., and G. Govers, Two-dimensional modelling of the within-field variation in rill and gully geometry and location related to topography, *Catena*, *29*, 283–306, 1997.

Desmet, P. J. J., J. Poesen, G. Govers, and K. Vandale, Importance of slope gradient and contributing area for optimal prediction of the initiation and trajectory of ephemeral gullies, *Catena*, *37*, 377–392, 1999.

Dietrich, W. E., and T. Dunne, The channel head, in *Channel Network Hydrology*, edited by K. Beven and M. J. Kirkby, pp. 175–219, John Wiley, New York, 1993.

Dietrich, W. E., C. J. Wilson, D. R. Montgomery, and J. McKean, Analysis of erosion thresholds, channel networks, and landscape morphology using a digital terrain model, *J. Geol.*, *101*, 259–278, 1993.

Dunne, T., and B. F. Aubry, Evaluation of Horton's theory of sheetwash and rill erosion on the basis of field experiments, in *Hillslope Processes*, edited by A. D. Abrahams, pp. 31–53, Allen and Unwin, Concord, Mass., 1986.

Engman, E. T., Roughness coefficients for routing surface runoff, *J. Irrig. Drain. Eng.*, *112*(1), 39–53, 1986.

Foster, G. R., L. J. Lane, M. A. Nearing, S. C. Finkner, and D. C. Flanagan, Erosion component, in *USDA—Water Erosion Prediction Project: Hillslope Profile Model Documentation*, edited by L. J. Lane and M. A. Nearing, pp.10.1–10.12, *NSERL Rep. 2*, Natl. Soil Erosion Res. Lab., Agric. Res. Serv., U. S. Dep. of Agric., West Lafayette, Ind., 1989.

Gessler, J., Beginning and ceasing of sediment motion, in *River Mechanics*, edited by H. W. Shen, chap. 7, pp.7.1–7.22, Colo. State Univ., Fort Collins, 1971.

Gupta, H. V., S. Sorooshian, and P. O. Yapo, Toward improved calibration of hydrologic models: Multiple and noncommensurable measures of information, *Water Resour. Res.*, *34*(4), 751–763, 1998.

Horton, R. E., Erosional development of streams and their drainage basins: Hydrophysical approach to quantitative morphology, *Geol. Soc. Am. Bull.*, *56*, 275–370, 1945.

Ijjasz-Vasquez, E. J., and R. L. Bras, Scaling regimes of local slope versus contributing area in digital elevation models, *Geomorphology*, *12*(4), 299–311, 1995.

Julien, P. Y., and D. B. Simons, Sediment transport capacity of overland flow, *Trans. ASAE*, *28*(3), 755–762, 1985.

Megahan, W. F., Erosion over time on severely disturbed granitic soils: A model, *For. Serv. Res. Pap. INT-156*, 14 pp., Intermt. Res. Stn., For. Serv., U.S. Dep. of Agric., Ogden, Utah, 1974.

Megahan, W. F., and W. J. Kidd, Effect of logging roads on sediment production rates in the Idaho Batholith, *For Serv. Res. Pap. INT-123*, 14 pp., Intermt. Res. Stn., For. Serv., U.S. Dep. of Agric., Ogden, Utah, 1972.

Megahan, W. F., and J. L. Clayton, Saturated hydraulic conductivities of granitic materials of the Idaho Batholith, *J. Hydrol.*, *84*(1–2), 167–180, 1986.

Miller, M. C., I. N. McCave, and P. D. Komar, Threshold of sediment motion under unidirectional currents, *Sedimentology*, *24*, 507–527, 1977.

Montgomery, D. R., Road surface drainage, channel initiation, and slope instability, *Water Resour. Res.*, *30*(6), 1925–1932, 1994.

Montgomery, D. R., Erosional processes at an abrupt channel head: Implications for channel entrenchment and discontinuous gully formation, in *Incised River Channels: Processes, Forms, Engineering and Management*, edited by S. E. Darby and A. Simon, pp. 247–276, John Wiley, New York, 1999.

Montgomery, D. R., and W. E. Dietrich, Where do channels begin, *Nature*, *336*, 232–234, 1988.

Montgomery, D. R., and W. E. Dietrich, Source areas, drainage density, and channel initiation, *Water Resour. Res.*, *25*(8), 1907–1918, 1989.

Montgomery, D. R., and W. E. Dietrich, Channel initiation and the problem of landscape scale, *Science*, *255*, 826–830, 1992.

Montgomery, D. R., and W. E. Dietrich, Landscape dissection and drainage area-slope thresholds, in *Process Models and Theoretical Geomorphology*, edited by M. J. Kirkby, pp. 221–246, John Wiley, New York, 1994.

Montgomery, D. R., and E. Foufoula-Georgiou, Channel network source representation using digital elevation models, *Water Resour. Res.*, *29*(12), 3925–3934, 1993.

Nearing, M. A., J. R. Simanton, L. D. Norton, S. J. Bulygin, and J. Stone, Soil erosion by surface water flow on a stony, semiarid hillslope, *Earth Surf. Processes Landforms*, *24*, 677–686, 1999.

Prosser, I. P., and B. Abernethy, Predicting the topographic limits to a gully network using a digital terrain model and process thresholds, *Water Resour. Res.*, *32*(7), 2289–2298, 1996.

Prosser, I. P., and W. E. Dietrich, Field experiments on erosion by overland flow and their implication for a digital terrain model of channel initiation, *Water Resour. Res.*, *31*(11), 2867–2876, 1995.

Prosser, I. P., and M. Soufi, Controls on gully formation following forest clearing in a humid temperature environment, *Water Resour. Res.*, *34*(12), 3661–3671, 1998.

Rodriguez-Iturbe, I., The geomorphological unit hydrograph, in *Channel Network Hydrology*, edited by K. Beven and M. J. Kirkby, pp. 43–68, John Wiley, New York, 1993.

Rouhipour, H., C. W. Rose, B. Yu, and H. Ghadirr, Roughness coefficients and velocity estimation in well-inundated sheet and rilled overland flow without strongly eroded bed forms, *Earth Surf. Processes Landforms*, *24*, 233–245, 1999.

Shields, A., Application of similarity principles and turbulence research to bed-load movement (in German), No. 26, Preuss. Vers. Anst. Wasserb. Schiffb., Berlin, 1936. (English translation available as *Hydrodyn. Lab. Publ. 67*, Hydrodyn. Lab., Calif. Inst. of Technol., Pasadena.).

Smith, T. R., and F. P. Bretherton, Stability and the conservation of mass in drainage basin evolution, *Water Resour. Res.*, *8*(6), 1506–1529, 1972.

Tarboton, D. G., A new method for the determination of flow directions and contributing areas in grid digital elevation models, *Water Resour. Res.*, *33*(2), 309–319, 1997.

Tarboton, D. G., R. L. Bras, and I. Rodriguez-Iturbe, A physical basis for drainage density, *Geomorphology*, *5*, 59–76, 1992.

Tiscareno-Lopez, M., V. L. Lopes, J. L. Stone, and L. J. Lane, Sensitivity analysis of the WEPP watershed model for rangeland applications, II, Channel processes, *Trans. ASAE*, *37*(1), 151–158, 1994.

Tucker, G. E., and R. L. Bras, Hillslope processes, drainage density, and landscape morphology, *Water Resour. Res.*, *34*(10), 2751–2764, 1998.

Willgoose, G., and R. L. Bras, A coupled channel network growth and hillslope evolution model, 1, Theory, *Water Resour. Res.*, *27*(7), 1671–1684, 1991a.

Willgoose, G., R. L. Bras, and I. Rodriguez-Iturbe, A physical explanation of an observed link area-slope relationship, *Water Resour. Res.*, *27*(7), 1697–1702, 1991b.

Willgoose, G. R., A physically based channel network and catchment evolution model, Ph.D. thesis, 464 pp., Mass. Inst. of Technol., Cambridge, 1989.

Woolhiser, D. A., R. E. Smith, and D. C. Goodrich, KINEROS, a kinematic runoff and erosion model; documentation and user manual, *ARS-77*, 130 pp., Agric. Res. Serv., U.S. Dep. of Agric., Tucson, Ariz., 1990.

Yalin, M. S., and E. Karahan, Inception of sediment transport, *J. Hydraul. Div. Am. Soc. Civ. Eng.*, *105*, 1433–1443, 1979.

Yen, B. C., Hydraulic resistance in open channels, in *Channel Flow Resistance: Centennial of Manning's Formula*, edited by Yen, B. C., pp. 1–136, Water Resour. Publ., Highlands Ranch, Colo., 1992.

E. Istanbulluoglu, Department of Civil and Environmental Engineering, Massachusetts Institute of Technology, 77 Massachusetts Avenue, Room 48-114, Cambridge, MA 02139, USA. (erkan@mit.edu)

C. Luce, Rocky Mountain Research Station, U.S. Forest Service, Boise, Idaho 83702, USA. (cluce@fs.fed.us)

R. T. Pack and D. G. Tarboton, Civil and Environmental Engineering Department, Utah State University, 4110 Old Main Hill, Logan, UT 84322-4110, USA. (rtpack@cc.usu.edu; dtarb@cc.usu.edu)